



Bulletin of the Mineral Research and Exploration

<http://bulletin.mta.gov.tr>



Evolution of slab tearing-related high potassium volcanism: Petrogenetic data from the Emirdağ and İncehisar volcanic units

Selin BİLGİÇ GENCER^a, Sibel TATAR ERKÜL^{b*} and Fuat ERKÜL^c

^a*Çiftay Construction, Divriği Iron Ore Mine, Sivas, Turkey*

^b*Akdeniz University, Department of Geological Engineering, Antalya, Turkey*

^c*Akdeniz University, Vocational School of Technical Sciences, Antalya, Turkey*

Research Article

Keywords:

Afyon high potassium volcanism, Sr-Nd isotopes, Slab tearing, Slab roll-back.

ABSTRACT

Volcanism that has been active since the early Miocene along a N-S trending line from Eskişehir to Isparta displays calc-alkaline and alkaline character and is closely associated with slab tearing processes. However, the geodynamic setting of these volcanic units between Afyon and Emirdağ is still poorly known. In this study, petrological characteristics of the Emirdağ and İncehisar volcanic units have been investigated using petrography, whole-rock geochemistry and Sr-Nd isotopes. The Emirdağ and İncehisar volcanic units overlap the Seydileğnimbrites. The Emirdağ volcanic unit is trachyandesite and the İncehisar volcanic unit is trachyte, basaltic trachyandesite and trachydacite in composition. The Emirdağ volcanic unit displays calc-alkaline character, while the İncehisar volcanic unit is alkaline but the rocks from both the units have shoshonite character defined by their high K₂O contents. The Emirdağ volcanic unit has ⁸⁷Sr/⁸⁶Sr ratios of 0.706790-0.706284 and ¹⁴³Nd/¹⁴⁴Nd ratios of 0.512472-0.512463, while these ratios in the İncehisar volcanic unit are of 0.707650-0.706527 and 0.512464-0.512424, respectively. Data revealed by this study indicate that these volcanic units were affected by crustal contamination, fractional crystallization and magma mixing. Rising of asthenosphere in the region due to the extensional regime in the Early Miocene appears to have caused formation of volcanism that pass from calc-alkaline to alkaline in character. The Emirdağ and İncehisar volcanic units are the products of the volcanism that developed in the late stages of southward slab roll-back and in the extensional regime prior to the slab tearing event.

Geliş Tarihi: 12.11.2019

Kabul Tarihi: 24.02.2020

1. Introduction

Magmatic rocks in Western Anatolia are observed in belts that occurred from north to south beginning in the Eocene until the middle Miocene following closure of the northern branch of the Neotethys. Volcanic and plutonic rocks developed in this time interval have high-K calc-alkaline, shoshonitic and ultrapotassic character. Though different opinions about the source of magmatism, stated to have

developed under compressional or extensional regime, have been proposed such as delamination-related orogenic collapse, slab roll-back of subducted oceanic slab at different rates and back-arc extension, the idea that the southward roll-back of the African plate being subducted to the north caused core complex formation and development of magmatic belts has gained acceptance (Seyitoğlu and Scott, 1996; Dewey, 1988; Agostini et al., 2008; Dilek and Altunkaynak, 2009). Volcanism in the region

Citation info: Gencer, S.B., Erkül, S.T., Erkül, F. 2020. Evolution of slab tearing-related high potassium volcanism: Petrogenetic data from the Emirdağ and İncehisar volcanic units. Bulletin of the Mineral Research and Exploration 163, 167-185.
<https://doi.org/10.19111/bulletinofmre.693353>.

*Corresponding author: Sibel TATAR ERKÜL, sibel582@gmail.com

developed along NE-SW striking fault systems under the effect of transtensional regime within nearly E-W belts (Erkül et al., 2005a, b, 2006; Ersoy et al., 2008; Karaoğlu et al., 2010; Karaoğlu and Helvacı, 2012, 2014). Deep seismic tomography studies in recent years indicates that the African oceanic slab subducted under Anatolia has very fragmented structure and that slab-tear processes were effective in formation of orogenic and anorogenic volcanism in the region (Biryol et al., 2011; Mahatsente et al., 2017; Portner et al., 2018). This prediction is largely supported by geochemical and geochronologic data (Karaoğlu and Helvacı, 2014; Prelević et al., 2015). The volcanic units located in the eastern section of the magmatic belts in Western Anatolia extend nearly 250 km along a line from Kırka, Afyon and Isparta and give varying

ages from the early Miocene to the present day (Keller and Villari, 1972; Besang et al., 1977; Sunder, 1980; Keller, 1983; Yağmurlu et al., 1997; Savaşçın and Oyman, 1998; Akal, 2003, 2008; Platevoet et al., 2008; Elitok et al., 2010; Prelević et al., 2015; Seghedi and Helvacı, 2016) (Figure 1a, b). Volcanic rocks in the Kırka, Afyon and Isparta regions occur to have more pronounced alkaline character compared to Miocene high potassium volcanic units in Western Anatolia (Francalanci et al., 2000; Innocenti et al., 2005; Prelević et al., 2010, 2012). These volcanic units developed in parallel with regional convergence direction above the intersection between the Cyprus and Hellenic subduction zones (Yağmurlu et al., 1997; Savaşçın and Oyman, 1998; Dilek and Altunkaynak, 2009). As a result, many studies attributed magmatic

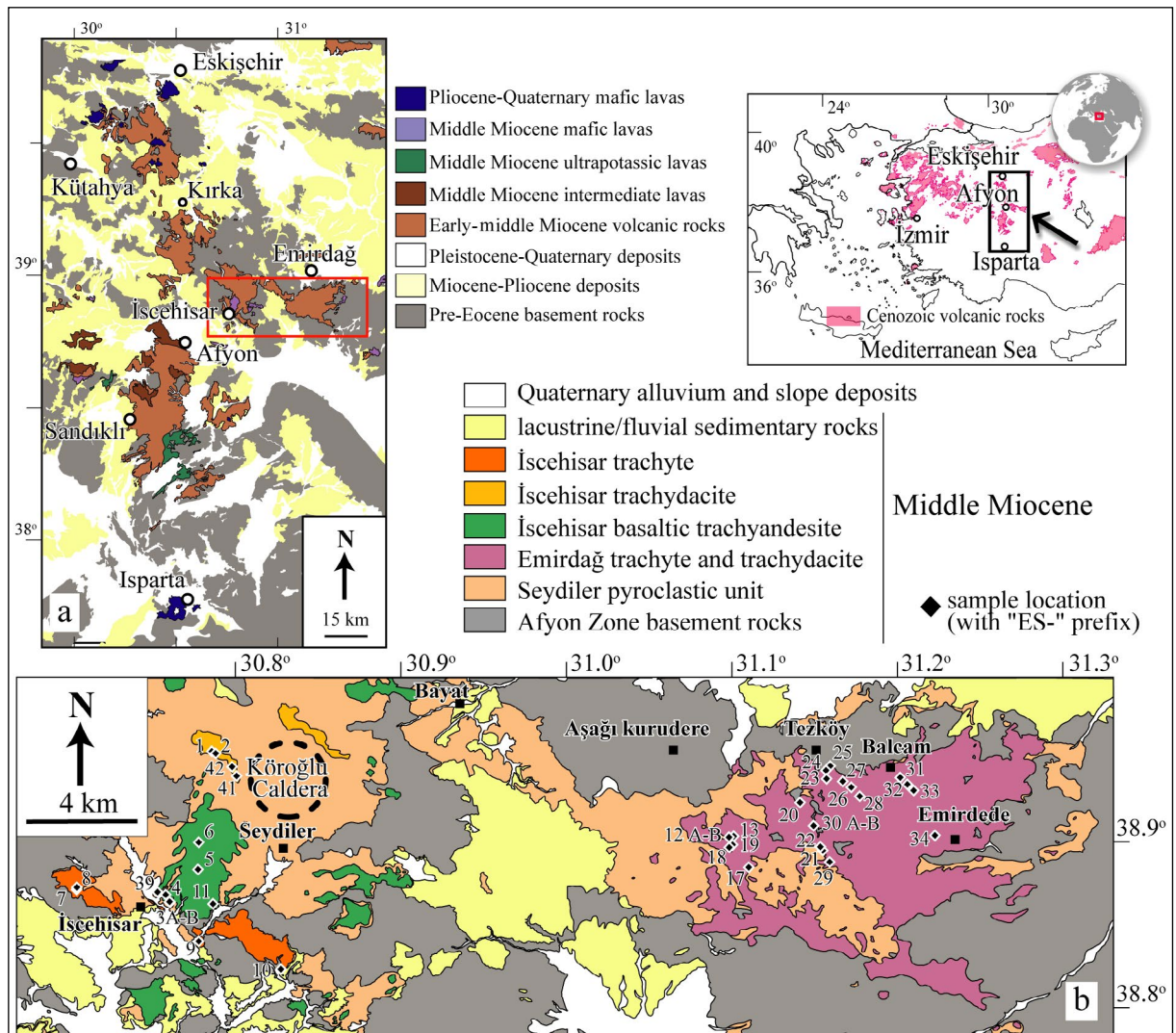


Figure 1- a) Simplified geologic map showing distribution of volcanic rocks outcropping along the Eskişehir-Afyon-Isparta line. Adapted from the 1/500.000 scale MTA (2002) geologic map. b) Geologic map of the İscehisar and Emirdağ volcanic units.

activity to the asthenospheric heat source owing to mantle upwelling between these two subducted plates (Yağmurlu et al., 1997; Savaşçın and Oyman, 1998). Petrological studies, especially on ultrapotassic volcanic rocks, indicate that these rocks probably derived from a highly metasomatized mantle source and the asthenospheric contribution increased with an advancing slab tear (Aydar and Beyhan, 1995; Aydar et al., 1998; Savaşçın and Güleç, 1990; Francalanci et al., 1990, 2000; Innocenti et al., 2005; Akal, 2008; Prelević et al., 2015; Erkül et al., 2019).

There are many studies to decipher the magma source characteristics of calc-alkaline, alkaline, shoshonitic and ultrapotassic volcanism developing along a N-S line extending from Eskişehir to Isparta (Aydar et al., 1996, 2003; Savaşçın and Oyman, 1998; Tonarini et al., 2005; Kumral et al., 2006; Çoban and Flower, 2006; Dilek and Altunkaynak, 2009; Doğan Külahcı et al., 2016; Prelević et al., 2010, 2012, 2015). However, the relationships between geodynamic processes of slab roll-back and tear, and the magma sources remain unknown for volcanic units extending on a NW-SE line from north of Afyon to Emirdağ regions. Within the scope of this study, geology, petrography, whole rock geochemistry and Sr-Nd isotope geochemistry of the Emirdağ and İsehisar volcanic units were investigated in an attempt to contribute to understanding the geodynamic evolution of the region.

2. Methods

A variety of analytical studies were performed to-define the geological characteristics and mineralogic-petrographic, geochemical and isotopic composition of the Emirdağ and İsehisar volcanic units. Collection of fresh or, if possible, least weathered samples was completed for petrographic identification, characterising all facies and geochemistry of the volcanic units. Samples taken from the Emirdağ and İsehisar volcanic units were investigated in terms of mineralogic composition and textural characteristics. After petrographic investigations, selected samples were broken to less than 0.4 cm size with the aid of a jaw crusher, then ground to less than 200 mesh size with a tungsten carbide vibrating mill. Whole-rock major and trace element analyses were completed for 28 chosen samples in ACME Laboratories, Vancouver, Canada. During major and trace element analyses, two

hundred milligrams rock powder was mixed with 1.5 g LiBO₂ fuser in a graphite bowl. Later the mixture was heated at 1050°C for 15 minutes in an oven. The melted samples were dissolved in 5% HNO₃ acid. Correction calculations used international standards and blank sample measurements. For major and some trace elements (Ba, Nb, Ni, Sr, Sc, Y, Zr), solutions were loaded into an ICP Emission Spectrometer and measured (Jarrel Ash AtomComb 975). For measurement of rare earth elements, solutions were loaded into an ICP Mass Spectrometer and measured (Perkin-Elmer Elan 6000). Sensitivity for major elements was less than 2%, while it was better than 10% for trace elements.

Seven samples representing the volcanic units had strontium and neodymium isotope analyses performed in Middle East Technical University, Radiogenic Isotope Laboratory. During measurement of Sr-Nd isotope ratios, TLM-ARG-RIL-01 (Sr Isotope Ratio Analysis Experiment Procedure) and TLM-ARG-RIL-02 (Nd Isotope Ratio Analysis Experiment Procedure) were applied. Details of these procedures are given in Köksal and Göncüoğlu (2008). Weighing, chemical solution and chromatography procedures were completed under clean laboratory conditions to 100 cleaning standards with ultra-pure water and chemicals. Approximately 80 mg of each rock powder sample was weighed and transferred to PFA bottles. Samples were left in 4 mL 52% HF for 4 days on a 160 °C heating table until fully dissolved. Samples dried on the heating table were first dissolved in 4 mL 6 NHCl for one day. Samples were later evaporated on the heating table again and placed in 1 mL 2.5 NHCl and prepared for chromatography. For strontium, Teflon columns were separated using 2.5 NHCl acid at 2 mL with Bio Rad AG50 W-X8 100-200 mesh resin. After collecting strontium, 6 NHCl and rare earth element fractions were collected. Strontium was loaded to single Re filaments on Ta-activator and 0.005 NH₃PO₄ and measured in static mode.

⁸⁷Sr/⁸⁶Sr data were normalized to ⁸⁶Sr/⁸⁸Sr = 0.1194. During measurements, Sr NBA 987 standard was measured as 0.710251±10 (n=2). Neodymium was separated from the other rare earth elements using 0.22 NHCl acid in Teflon columns with 2 mL HDEHP (bis-ethyexyl phosphate)-covered biobeads by passing through Bio-Rad resin. The separated neodymium was measured in static mode using the double-filament

technique loaded on refilaments with 0.005 NH₃PO₄. During analyses, ¹⁴³Nd/¹⁴⁴Nd data were normalized to ¹⁴⁶Nd/¹⁴⁴Nd = 0.7219, while the Nd La Jolla standard was measured as 0.511851±10 (n=2). No bias correction was made for the measurement results for strontium and Nd isotope ratios. Measurements were completed with multiple collection using Triton Thermal Ionisation Mass Spectrometer (Thermo-Fisher). Analytic uncertainty was at 2 sigma level. Results obtained for major, trace and isotope geochemistry were evaluated using GCDkit software (Janousek et al., 2006).

3. Geology

Lithostratigraphic units around the Emirdağ and İncehisar areas comprise, from oldest to youngest, basement rocks of the Palaeozoic metamorphic rocks and Afyon Zone, Miocene volcanic units and lacustrine/fluvial sedimentary deposits. The Afyon Zone around İncehisar and Emirdağ was formerly named the Afyon Metamorphics, consisting of Palaeozoic low-grade metamorphic rocks of phyllite, mica schist and quartzite with marble successions and Mesozoic carbonate and chert sequences (Metin et al., 1987).

Fluvial and lacustrine sedimentary rocks are located southwest and southeast of İncehisar and west and southwest of Emirdağ (Metin et al., 1987). The sequence covers metamorphic basement with basal conglomerate and continues upward into volcanoclastic rocks with clay and marl intercalations and ends with lacustrine limestone on top of the succession.

Thick pyroclastic deposits around Emirdağ and İncehisar were named the Seydiler tuff/agglomerate (Metin et al., 1987) and Seydiler Ignimbrite (Aydar et al., 1998) in previous studies, comprising nearly 200-250-metres thick pyroclastic layers dominated by ignimbrites, occasionally intercalated with epiclastic sediments passing laterally into lacustrine and fluvial sediments in distal sections. Trachydacite, trachyte and basaltic trachyandesites occurred on stratigraphically upper levels of the pyroclastic rocks around İncehisar and Emirdağ areas. Two samples from the İncehisar volcanic unit were dated 15.37 and 16.08 Ma using the ⁴⁰Ar/³⁹Ar method (Prelević et al., 2012). These ages are comparable to ⁴⁰Ar/³⁹Ar ages of the Emirdağ volcanic unit (16.5 My, unpublished). The volcanic

rocks occurring as domes, dykes and massive lava flows were named as the Emirdağ volcanic unit and İncehisar volcanic unit in this study.

The Emirdağ volcanic unit is represented by domes, dykes and lava flows. Domes and lava flows overlap intercalations of ignimbrites, block and ash flow and debris flow deposits (Figure 2 a-c). Domes and lava flows contain large sanidine phenocrysts with lengths reaching up to 4 cm (Figure 2d). Dykes are lithologically similar to lava flows and domes, strike NW-SE in direction and their thickness reaches up to 2 metres.

Around İncehisar, lava flows are relatively more common than domes (Figure 2e). Lava flows occur above ignimbrites that are locally overlain by thin and cross-bedded fluvial sediments, suggesting a short time gap after deposition (Figure 2f). Massive lava flows are recognised by blackish, pinkish, dark grey colours, occasional weathering, breccia structure, flow bands and abundant vesicles. Their thickness reaches up to 50 metres.

4. Mineralogy-Petrography

The Emirdağ volcanic unit is mainly trachyandesite, trachyte and trachydacite in composition but trachydacites also occur. Trachyandesites are distinguished by the abundance of amphibole and biotite phenocrysts, while trachytes contain large sanidine crystals. Trachydacites are recognised by quartz phenocrysts in hand specimen. All rocks have hyalopilitic and occasional microlitic flow texture and consist of quartz, plagioclase, sanidine, biotite, augite, kaersutite, hornblende and apatite minerals. Large quartz phenocrysts are anhedral and display embayments, representing renewed reactions with magma. Biotites contain plagioclase and groundmass inclusions. Reddish-brownish kaersutite crystals are euhedral, opacified along their rims and are commonly embayed. Zoned plagioclase phenocrysts and melt inclusions in olivine, pyroxene and biotite are suggestive of magma mixing processes (Figure 3a-h).

The İncehisar volcanic unit is formed by contrasting mineral assemblages owing to varying compositions of lavas. Basaltic trachyandesites that consist of plagioclase, olivine, augite, kaersutite and biotite phenocrysts are defined by hyalopilitic and

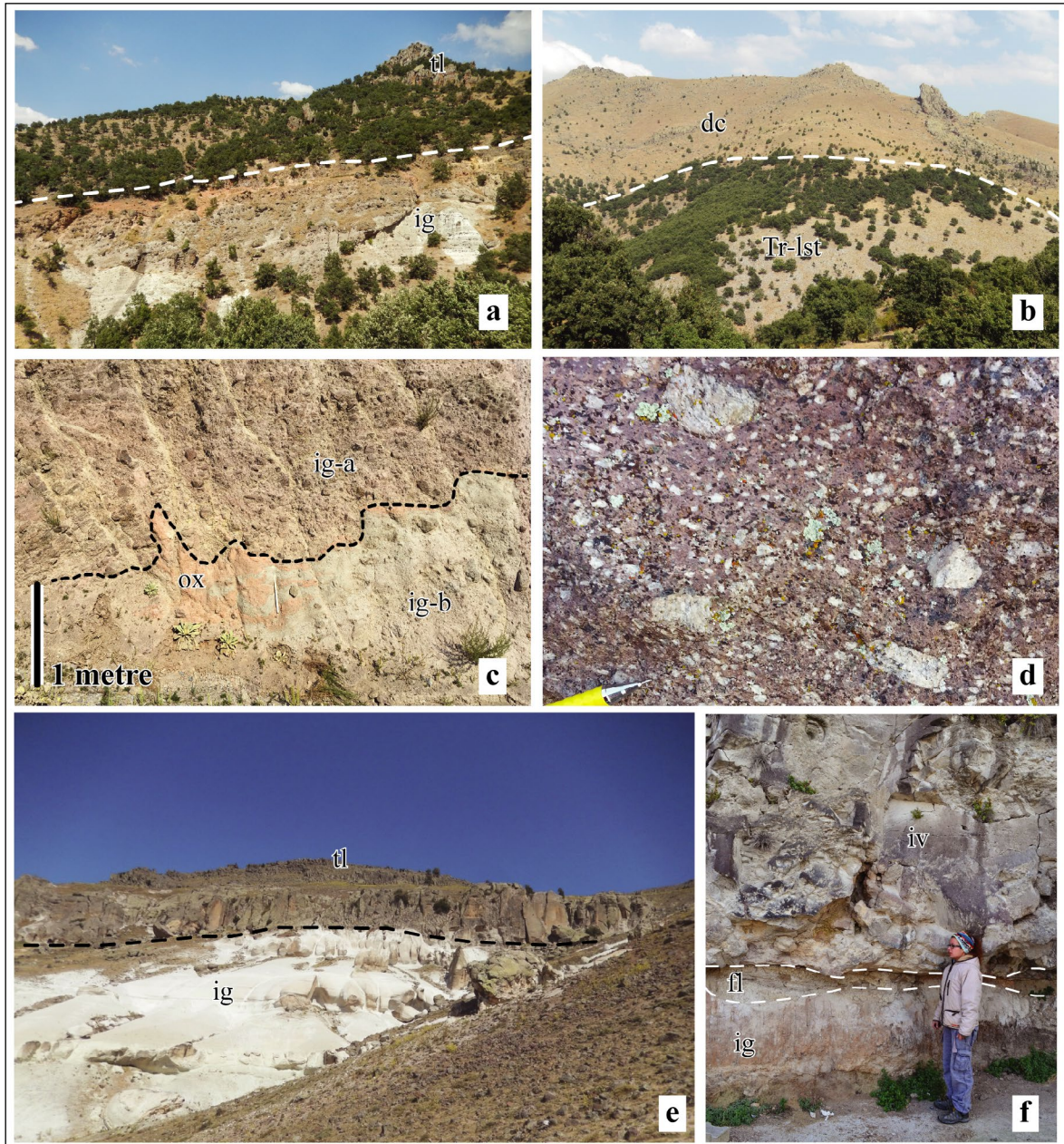


Figure 2- a) Trachydacites (tl) above ignimbrites and block and ash flow deposits near Emirdağ (31.148°/38.926°), b) trachydacite dome and dyke system emplaced by cutting Triassic recrystallized limestones south of Tezköy. Abbreviations; dc: dome and dyke complex, Tr-lst: Triassic limestones (31.154°/ 38.922°), c) contact between lithic-rich (ig-a) and lower lithic-poor (ig-b) pyroclastic flow deposits within Emirdağ volcanic unit and oxidized (ox) zone suggesting hot emplacement of the overlying ignimbrites (31.116°/38.915°), d) large sanidine crystals observed in a pink-coloured matrix in trachydacites of the Emirdağ volcanic unit. Length of sanidines reach up to 4 cm (31.104°/38.901°), e) columnar-jointed trachydacites conformably above light-coloured diffusely stratified ignimbrites (ig) (30.780°/38.951°) and f) basaltic trachyandesites of the İscehisar volcanic unit (iv) above ignimbrites (ig) and thin-bedded fluvial sediments (fl) in İscehisar area (30.752°/38.860°).

occasional trachytic texture. Olivine phenocrysts display common iddingsitization, carbonatization and opacification. Clinopyroxene phenocrysts, locally occurring as cumulates, are more common compared to orthopyroxene. Pyroxenes with polysynthetic

twinning have embayed margins, indicating interaction with magma. Trachytes comprise plagioclase, olivine, biotite, augite and kaersutite phenocrysts and microlites. They have typical trachytic texture and occasional radial microlite

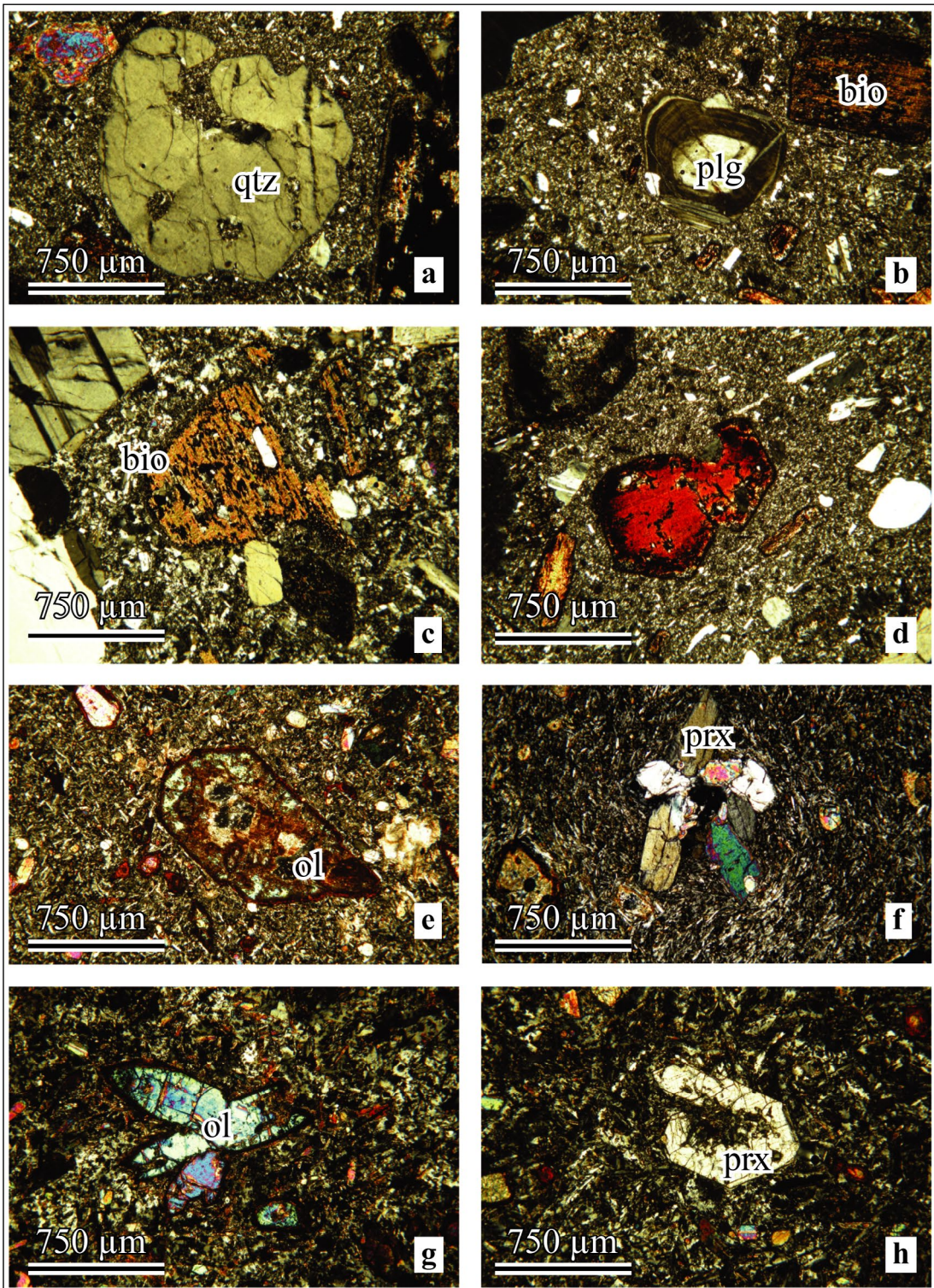


Figure 3- a) Embayed quartz phenocrysts within trachydacites of the Emirdağ volcanic unit, b) zoned plagioclase phenocrysts within trachydacites of the Emirdağ volcanic unit, suggesting the presence of magma mixing processes, c) enclosed plagioclase crystals and matrix in biotite (bio) phenocrysts having opaque rim observed in trachydacites of the Emirdağ volcanic unit, d) a reddish, embayed kaersutite phenocryst with opacified rims in trachydacites of the Emirdağ volcanic unit, e) iddingsitized and opacified subhedral olivine (ol) phenocrysts within basaltic trachyandesites of the İncehisar volcanic unit, f) Clinopyroxene (prx) cumulates in basaltic trachyandesites of the İncehisar volcanic unit, g) Olivine cumulates in basaltic trachyandesites of the İncehisar volcanic unit and h) Embayed pyroxene phenocrysts in trachytes of the İncehisar volcanic unit.

growths are observed. Ferromagnesian minerals of biotite, augite and kaersutite are largely altered to opaque phases and olivine phenocrysts are almost completely iddingsitized. Basaltic trachyandesites have almost the same mineralogical composition as trachytes whilst they may be texturally contrasting. Trachyandesites commonly exhibit hyalopitic texture. Minor amount of olivine phenocrysts is almost completely iddingsitized. Kaersutites are in the form of laths and are altered to opaque phases. Augites contain common matrix inclusions. Trachydacites comprise plagioclase, augite, kaersutite, biotite and hornblende phenocrysts. Plagioclase crystals are in the form of long thin laths shaped. Kaersutite and augite phenocrysts are largely altered to opaque phases. In the lava flows of the İncehisar volcanic unit, matrix inclusions within pyroxene and olivine phenocrysts indicate the effects of magma mixing processes.

5. Geochemistry

After petrographic studies, major and trace element analyses of 27 fresh whole-rock samples have been performed in order to, classify and define petrogenetic features of the volcanic rocks exposed in the Emirdağ and İncehisar regions. Analytical results are given in table 1. Attempts were made to determine the geochemical characteristics of early-middle Miocene volcanism using classification and tectono-magmatic discrimination diagrams. On the total alkali-silica diagram (Figure 4a), samples of the İncehisar volcanic unit fall in the basaltic trachyandesite, trachyte and trachydacite fields, while samples from the Emirdağ volcanic unit fall in the trachyandesite and trachyte-tachydacite transition. According to the alkaline-subalkaline differentiation diagram of Le Bas et al. (1986), the İncehisar volcanic unit is alkaline, while trachydacites from the Emirdağ volcanic unit are subalkaline in character. According to Peccerillo and Taylor's (1976) K_2O versus SiO_2 diagram, the İncehisar and Emirdağ volcanic units have shoshonitic character (Figure 4b). $Mg\#$ values vary from 46 to 75 for the İncehisar volcanic unit and from 26 to 57 for the Emirdağ volcanic unit. Volcanic rocks with $MgO > 3$, $K_2O > 3$, $K_2O/Na_2O > 2$ and $(K_2O+Na_2O)/Al_2O_3 > 1$ were defined as ultrapotassic by Foley et al. (1987). Samples from the İncehisar and Emirdağ volcanic units were assessed according to the criteria recommended by Foley et al. (1987).

Samples from the Emirdağ volcanic unit have K_2O and MgO contents varying from 4.37 to 6.09 wt.% and 0.71 to 3.90 wt.%, while samples from the İncehisar volcanic unit have 4.34-8.61 wt.% and 3.28-9.44 wt.% for the same elements (Table 1). K_2O/Na_2O ratio for the Emirdağ volcanic samples is 1.34-2.30, while it varies between 1.61 and 5.38 in the İncehisar volcanic samples. $(K_2O+Na_2O)/Al_2O_3$ ratio is 0.48-0.61 for the Emirdağ volcanic samples and 0.46-0.88 for the İncehisar volcanic samples. The abovementioned element contents and ratios show that samples from the Emirdağ and İncehisar volcanic units cannot be classified as ultrapotassic.

The İncehisar volcanic unit differs from the Emirdağ volcanic unit with high SiO_2 , Fe_2O_3 , TiO_2 , MgO , K_2O , and P_2O_5 and low CaO and Na_2O values. The major and trace element contents of the İncehisar volcanic unit have great similarities to the geochemistry of lamprophyres described in Afyon and surroundings (Aydar et al., 2003; Dedeoğlu and Yılmaz, 2016) and on Kos (Soder, 2017). On the variation diagrams, Fe_2O_3 , CaO , MgO , TiO_2 , P_2O_5 , Rb , Th , U , and Nb increase with increasing SiO_2 content, while Al_2O_3 , Zr and V contents decrease. Na_2O is low in trachytes of the İncehisar volcanic unit, while is high in other volcanic rocks. K_2O is high in the İncehisar volcanic unit and is low in the Emirdağ volcanic unit (Figure 5a-l).

Primitive mantle normalized multi-element spider diagrams (Sun and McDonough, 1989) are given in figure 6. The Emirdağ and İncehisar volcanic samples appear to be depleted in Nb , Pb and Ti . Basaltic trachyandesites of the İncehisar volcanic unit are enriched in U , K and Zr , while trachytes are enriched in K and Zr . The Emirdağ volcanic unit is enriched in Cs , U and Nd (Figure 6a). Chondrite-normalized rare earth element spider diagrams (Boynton, 1984) are shown in figure 6b. All samples show depletion from light rare earth elements to heavy rare earth elements. Light rare earth elements have 200-500 times enrichment, while enrichment in heavy rare earth elements is from 7 to 15 times relative to Chondrite.

6. Sr-Nd Isotope Ratios

$^{87}Sr/^{86}Sr$ isotope ratios of the Emirdağ volcanic unit vary from 0.706790 to 0.706284, while

Table 1- Major and trace element content of bulk rock samples from Emirdag and Isehisar volcanic units.

Unit	Isehisar Volcanic Unit														Emirdag Volcanic Unit													
	Basaltic Trachyandesite/Trachyandesite							Trachyandesite							Trachydacite							Trachydacite						
	2	5	6	7	10	11	40	3B	9	8	4	41	1	15	16	17	21	27	31	32	33	14	18	19	23	29	35	
Major element (weight %)																												
SiO ₂	53.03	50.12	52.96	53.05	51.52	54.21	53.86	54.52	55.08	53.19	54.02	60.77	60.37	61.52	64.63	65.75	65.26	61.16	62.77	61.41	63.40	58.40	57.53	58.61	59.91	60.37	59.27	
TiO ₂	1.350	1.290	1.520	1.960	1.520	1.550	1.340	1.720	1.910	1.930	1.700	1.040	1.050	0.780	0.620	0.530	0.580	0.900	0.780	0.830	0.770	0.780	0.800	0.800	1.010	0.790	0.750	
Al ₂ O ₃	13.10	12.54	13.58	11.13	14.58	13.91	15.56	13.46	11.66	11.36	13.35	14.34	14.36	15.61	15.35	15.40	16.23	14.32	15.23	15.60	15.11	14.96	14.91	15.22	14.23	16.50	14.69	
Fe ₂ O ₃	7.190	7.530	7.290	5.990	8.150	7.170	7.660	7.400	6.480	6.090	7.310	4.590	4.760	5.370	4.560	3.770	4.080	4.900	4.830	5.070	4.920	5.730	5.750	6.010	5.090	5.420	5.770	
MgO	5.020	8.680	6.760	9.050	4.980	3.480	3.280	3.870	5.630	9.440	4.510	3.370	2.910	2.220	1.360	0.920	0.710	2.720	1.910	1.650	2.110	3.900	3.720	3.290	2.890	2.090	3.730	
CaO	7.440	7.320	6.660	5.470	8.790	6.410	6.880	5.870	5.620	5.400	6.270	4.460	4.740	4.470	3.400	3.120	2.460	4.810	3.750	3.680	4.060	6.060	5.890	5.260	4.960	4.120	5.960	
Na ₂ O	2.100	1.930	2.160	2.510	2.330	2.220	2.790	2.100	1.600	2.230	2.110	2.810	2.770	3.270	3.230	3.270	2.980	2.770	3.040	3.020	3.040	2.980	2.900	2.920	2.650	3.080	2.930	
K ₂ O	6.160	4.830	5.840	6.490	4.340	5.990	4.500	6.830	8.610	6.690	6.780	5.850	5.690	4.370	4.560	4.890	5.140	5.480	5.110	5.530	4.970	4.400	4.420	4.840	6.090	4.780	4.680	
MnO	0.120	0.130	0.110	0.100	0.100	0.090	0.100	0.080	0.110	0.090	0.090	0.070	0.080	0.070	0.090	0.070	0.060	0.090	0.090	0.090	0.090	0.090	0.120	0.090	0.060	0.070	0.090	
P ₂ O ₅	1.050	0.980	1.070	0.670	0.790	1.060	0.680	1.070	0.930	0.650	1.070	0.680	0.700	0.460	0.410	0.350	0.360	0.640	0.490	0.550	0.470	0.480	0.470	0.560	0.750	0.540	0.520	
LOI*	2.700	3.700	1.300	2.800	2.300	3.000	2.800	2.400	1.300	2.100	2.100	1.500	2.100	1.300	1.300	1.500	1.700	1.600	1.500	1.900	0.600	1.500	2.800	1.600	1.700	1.600	0.800	
TOTAL	99.26	99.21	99.29	99.37	99.41	99.15	99.46	99.36	98.99	99.33	99.36	99.49	99.51	99.48	99.48	99.53	99.52	99.45	99.50	99.39	99.52	99.30	99.31	99.25	99.41	99.39	99.25	
Trace Element (ppm)																												
Sc	24.00	23.00	22.00	17.00	28.00	22.00	22	22	18	17	22	13	14	13	10	8	8	15	12	13	12	15	16	16	15	13	16.00	
Cu	44.30	48.50	43.40	45.70	34.50	22.90	36.0	35.7	32.8	38.0	19.7	8.5	19.8	9.9	7.9	7.3	5.5	14.9	15.3	17.7	12.4	24.2	18.9	15.7	14.0	9.3	31.00	
Pb	4.200	3.600	4.200	11.10	4.100	2.300	3.8	5.2	12.7	9.5	1.0	0.8	0.9	2.4	1.7	3.8	4.5	3.6	2.6	2.4	1.4	8.3	2.7	4.7	8.7	5.6	11.20	
Zn	52.00	68.00	62.00	54.00	67.00	48.00	58	59	50	51	57	18	41	36	30	42	42	46	24	34	19	49	35	23	48	40	46.00	
Ni	31.20	280.9	122.2	328.5	56.60	97.40	109.1	85.3	90.2	319.2	69.4	5.7	8.7	8.8	4.0	3.4	2.7	7.6	10.4	13.5	5.7	12.3	14.4	7.5	8.6	4.2	10.00	
Co	55.40	97.90	62.30	64.20	47.30	53.00	71.1	136.5	49.4	55.3	114.5	69.2	43.4	70.2	53.6	53.8	105.1	55.4	58.8	57.2	52.7	54.1	51.7	53.0	60.4	46.6	54.30	
Mo	1.700	1.200	1.200	0.200	1.400	1.200	1.5	1.2	0.5	0.2	0.7	0.2	0.7	0.9	1.1	0.8	0.3	2.3	0.5	0.5	0.4	1.6	0.8	1	2.1	1	1.500	
Cs	6.500	8.000	3.300	9.300	3.000	4.900	14.3	10.6	3.2	11.0	5.8	8.8	8.5	15.9	18.0	18.2	19.9	13.7	16.5	14.3	17.9	10.6	10.8	12.5	15.5	11.1	9.600	
Nb	24.60	24.70	27.80	62.60	32.90	28.70	30.8	29.1	38.2	61.2	27.8	23.6	23.9	31.2	34.9	33.3	36.0	28.4	29.6	30.0	30.1	25.1	25.8	27.8	29.5	32.2	25.40	
Ga	17.50	17.00	18.20	20.00	16.50	18.20	17.6	20.5	20.0	19.4	18.6	18.9	18.0	17.7	18.3	18.0	18.6	17.9	17.2	18.4	17.7	17.3	17.6	18.3	18.2	18.9	16.90	

Table 1- (Continue).

V	182.0	171.0	174.0	132.0	237.0	158.0	165	153	113	142	177	85	100	111	92	74	69	116	92	114	89	131	128	113	122	124	127.0
W	195.6	421.8	256.1	226.1	165.5	196.0	234.2	441.3	158.0	148.2	304.5	354.2	182.2	380.6	324.3	337.3	414.9	336.0	329.3	315.8	278.6	261.8	228.1	240.0	300.5	251.8	243.0
Ba	2214	2709	2293	829.0	18700	3974	1695	1719	2157	1175	1791	1533	1539	1283	1445	1521	1571	1704	1358	1863	1219	2315	2325	2636	1886	2065	2636
Rb	206.3	129.1	158.5	332.7	129.6	167.2	141.7	211.7	258.3	333.8	211.7	218.0	214.9	190.6	227.9	243.3	250.4	220.4	214.2	214.6	210.8	166.9	168.9	187.0	231.0	189.2	166.6
Sr	1690	1019	1061	748.0	941.0	1170	934	990	1480	751	992	902	934	1313	1149	1063	955	1179	1203	1562	1166	1688	1624	1773	1257	1369	1782
Hf	14.90	13.90	17.90	31.80	12.90	18.10	12.3	19.6	27.1	31.3	18.8	13.6	13.2	8.0	8.0	6.8	7.5	11.0	9.7	10.4	10.4	7.3	7.2	8.4	12.6	8.4	7.700
Y	27.70	28.40	27.60	23.30	26.20	31.30	26.1	24.9	27.6	23.7	27.6	21.7	19.9	27.8	31.2	28.1	31.6	21.9	24.4	27.4	26.6	27.9	31.6	29.4	23.2	30.6	26.90
Zr	570.0	507.0	659.0	1174	470.0	674.0	477	725	947	1144	729	488	481	295	294	248	279	417	370	378	388	272	285	316	468	321	286.0
Th	18.40	14.40	16.10	25.10	14.80	17.20	15.8	15.2	32.0	23.6	14.7	17.2	16.5	42.0	53.2	44.9	47.3	35.2	35.4	43.9	39.7	45.4	43.9	55.4	33.2	45.8	52.20
U	6.500	5.000	5.000	2.600	2.500	5.300	4.9	5.1	5.1	1.9	5.2	6.8	6.7	17.3	18.1	13.7	17.7	17.2	15.5	16.0	15.6	17.3	12.5	18.6	16.1	18.6	18.40
Ta	1.400	1.500	1.600	3.600	1.900	1.800	1.7	1.7	2.1	3.7	1.8	1.7	1.9	2.6	2.9	2.8	3.0	2.1	2.3	2.3	2.3	2.0	1.9	2.0	2.0	2.5	2.100
La	80.10	63.00	71.00	105.9	56.70	77.90	64.2	70.9	162.2	102.9	71.9	64.0	62.4	110.3	119.3	93.2	04.1	76.5	87.3	114.9	96.3	122.0	131.6	139.5	80.3	123.7	133.9
Ce	166.4	124.2	146.0	230.7	112.5	159.3	122.0	144.2	337.1	223.3	148.1	129.8	125.7	193.9	217.6	166.4	178.7	146.3	167.3	219.9	186.2	229.7	229.4	257.6	151.3	222.5	257.2
Pr	19.05	14.39	16.72	25.52	12.62	18.18	13.80	17.19	38.87	25.03	17.28	14.42	14.14	20.89	22.62	17.54	19.44	15.83	18.48	22.65	19.31	24.64	26.33	27.32	16.16	24.06	27.16
Nd	73.30	55.20	62.30	93.40	46.50	68.30	51.1	66.5	144.3	91.0	68.0	55.2	53.7	71.8	80.3	62.9	68.0	56.6	68.0	79.1	69.7	88.9	97.9	99.2	59.7	87.0	96.70
Sm	12.87	10.37	10.44	13.65	8.520	11.64	8.58	11.16	19.56	13.21	11.34	8.75	8.87	11.34	12.67	9.72	10.49	9.01	10.53	11.74	10.79	13.78	15.30	15.26	9.83	13.78	15.13
Eu	3.120	2.560	2.570	2.860	2.230	2.670	2.14	2.58	4.10	2.72	2.64	1.99	1.97	2.58	2.60	2.06	2.23	2.07	2.41	2.65	2.47	3.12	3.42	3.32	2.29	2.95	3.350
Gd	9.370	8.300	8.460	9.330	7.070	9.130	6.98	8.31	12.48	9.06	8.45	6.76	6.43	8.53	9.51	7.41	7.91	6.99	7.47	8.40	7.86	9.78	11.15	10.61	7.19	9.75	10.16
Tb	1.190	1.080	1.110	1.110	0.990	1.190	0.96	1.04	1.31	1.08	1.10	0.87	0.84	1.10	1.18	0.99	1.06	0.89	0.95	1.03	0.98	1.10	1.24	1.24	0.88	1.19	1.170
Dy	5.800	5.600	5.760	5.620	5.110	5.850	5.06	5.22	5.91	5.10	5.81	4.25	4.05	5.52	6.12	4.98	5.54	4.53	4.87	5.01	4.78	5.57	6.17	5.75	4.40	5.99	5.680
Ho	0.970	1.000	1.000	0.820	0.940	1.080	0.92	0.90	0.92	0.83	0.95	0.68	0.68	0.98	1.08	0.91	1.02	0.76	0.88	0.91	0.86	0.88	1.06	0.95	0.83	1.04	0.880
Er	2.640	2.670	2.630	2.180	2.660	2.910	2.50	2.35	2.46	2.11	2.67	1.95	1.81	2.48	2.98	2.62	3.00	2.06	2.47	2.44	2.55	2.74	3.20	2.65	2.06	2.77	2.560
Tm	0.380	0.380	0.380	0.290	0.340	0.430	0.38	0.34	0.36	0.28	0.37	0.26	0.28	0.39	0.46	0.40	0.43	0.30	0.33	0.36	0.38	0.38	0.44	0.41	0.30	0.43	0.380
Yb	2.300	2.220	2.370	1.920	2.280	2.540	2.24	2.02	2.29	1.72	2.25	1.67	1.57	2.66	3.04	2.58	3.11	2.09	2.32	2.40	2.50	2.44	2.81	2.57	2.10	2.72	2.420
Lu	0.320	0.360	0.350	0.260	0.360	0.400	0.37	0.30	0.31	0.24	0.34	0.24	0.26	0.36	0.47	0.42	0.44	0.31	0.35	0.36	0.38	0.36	0.40	0.37	0.32	0.42	0.360
Mg#1	58.00	70.00	65.00	75.00	55.00	49.00	46.00	51.00	63.00	75.00	55.00	59.00	55.00	45.00	37.00	33.00	26.00	52.00	44.00	39.00	46.00	57.00	56.00	52.00	53.00	43.00	56.00

*LOI: loss on ignition

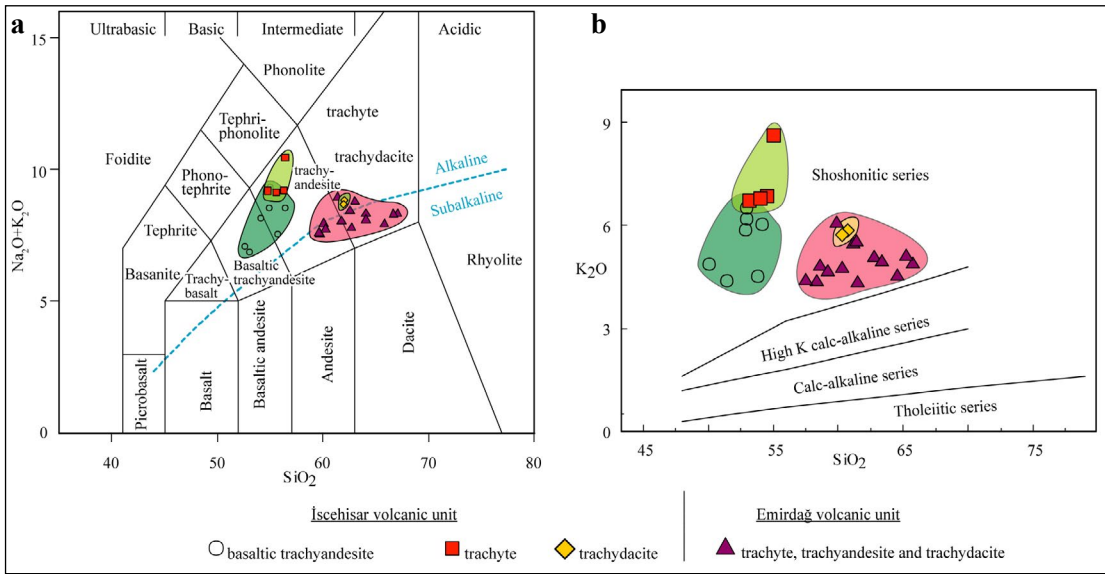


Figure 4- a) Total alkali- SiO_2 variation diagram (Le Bas et al., 1986) showing sample plots belonging to the İscehisar and Emirdağ volcanic units. Alkaline-subalkaline differentiation line taken from Irvine and Baragar (1971). b) Distribution of samples on K_2O - SiO_2 diagram (Peccerillo and Taylor, 1976).

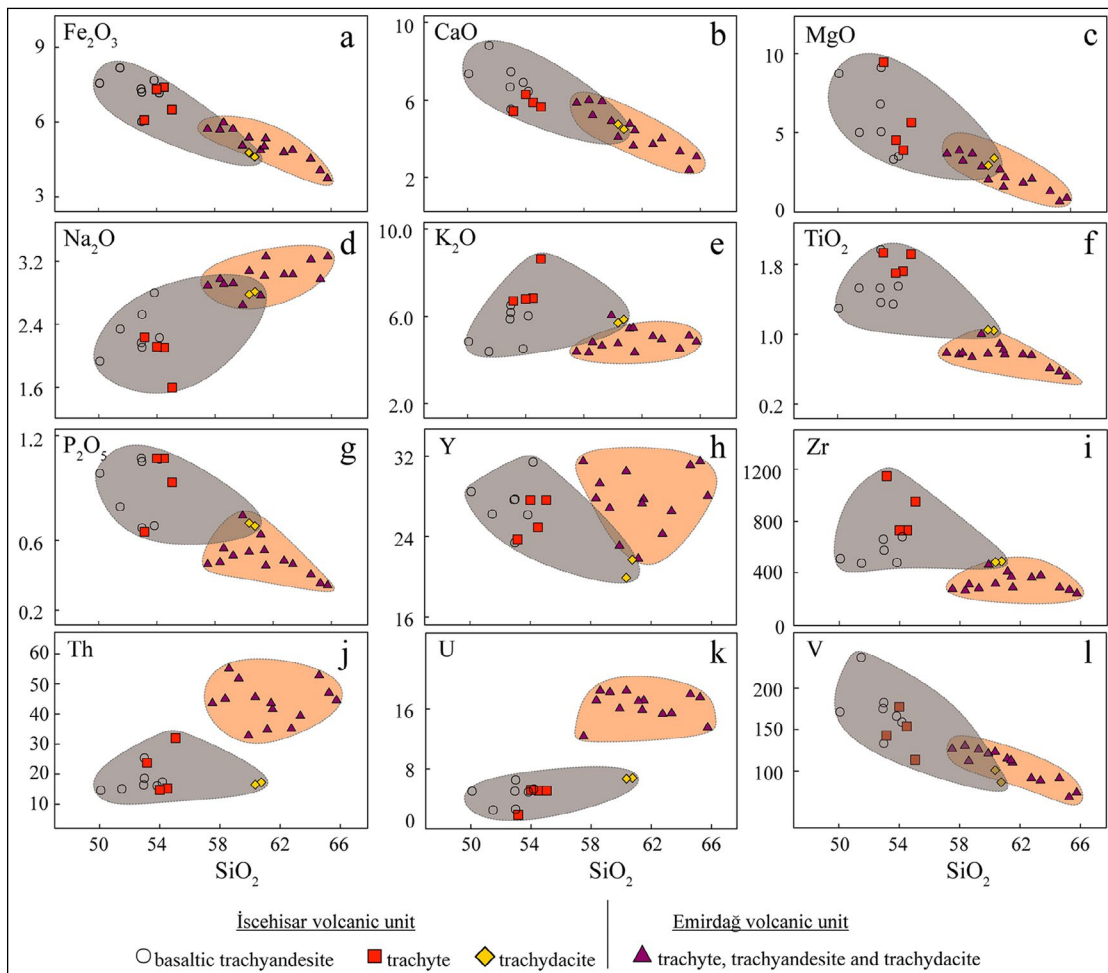


Figure 5- Major and trace element variation diagrams against SiO_2 for samples from İscehisar and Emirdağ volcanic units. Contents are weight % for major elements and ppm for trace elements.

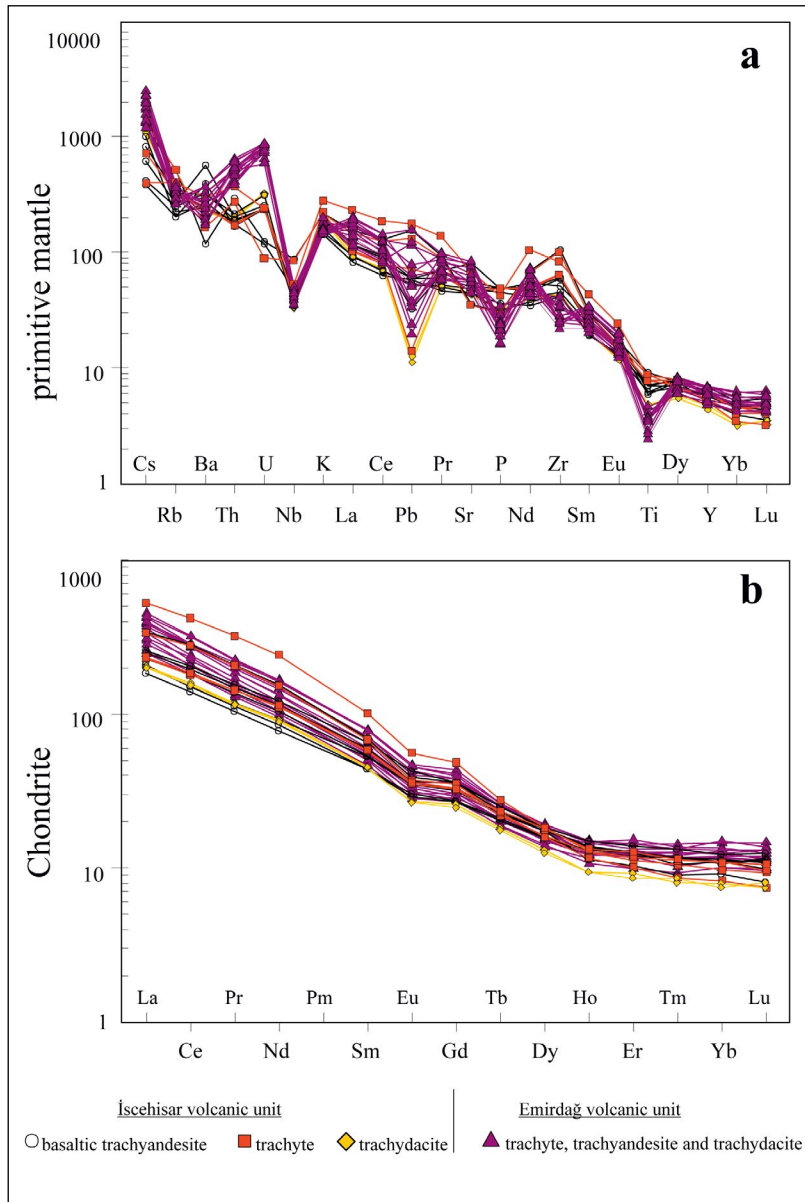


Figure 6- a) Spider diagrams normalized to primitive mantle (Sun and McDonough, 1989) and b) chondrite for samples from the İsehisar and Emirdağ volcanic units (Boynton, 1984).

$^{143}\text{Nd}/^{144}\text{Nd}$ isotope ratios is between 0.512472 and 0.512463. The same isotope ratios of the İsehisar volcanic unit are 0.707650-0.706527 and 0.512464-0.512424, respectively (Table 2) (Figure 7). The Sr and Nd isotope ratios for samples from the Emirdağ and İsehisar volcanic units are similar to the Sr-Nd isotope ratios of high-K and ultrapotassic volcanic rocks from Afyon and surroundings (Innocenti et al., 2005; Dilek and Altunkaynak, 2010; Chakrabarti et al., 2012; Prelević et al., 2012, 2015). When compared with silica-saturated and undersaturated volcanic

rocks of the Afyon volcanic complex, (Prelević et al., 2015), the Emirdağ and İsehisar volcanic units have overlapping $^{87}\text{Sr}/^{86}\text{Sr}$ and $^{143}\text{Nd}/^{144}\text{Nd}$ ratios.

7. Magma Source and Evolution Processes

The Emirdağ volcanic unit display a compositional variation from trachyandesite to trachydacite, the majority of the samples are trachydacite in composition. Most samples are calc-alkaline and

Table 2- Sr-Nd isotope ratios for bulk rock samples from the Emirdağ and İscehisar volcanic units.

Sample	Unit	Rock type	Rb (ppm)	Sr (ppm)	Nd (ppm)	⁸⁷ Sr/ ⁸⁶ Sr	Std. error	¹⁴³ Nd/ ¹⁴⁴ Nd	Std. error
ES-16	Emirdağ volcanic unit	Trachydacite	227.9	1148.6	80.3	0.706790	9	0.512463	2
ES-23		Trachydacite	231.0	1256.6	59.7	0.706284	6	0.512466	3
ES-31		Trachydacite	214.2	1203.1	68.0	0.706342	6	0.512472	3
ES-41	İscehisar volcanic unit	Trachydacite	218.0	902.7	55.2	0.707650	7	0.512424	3
ES-9		Trachyte	258.3	1479.8	144.3	0.706881	5	0.512454	3
ES-6		Basaltic Trachyandesite	158.5	1061.2	62.3	0.707514	5	0.512449	2
ES-10		Basaltic Trachyandesite	129.6	941.4	46.5	0.706527	5	0.512464	4

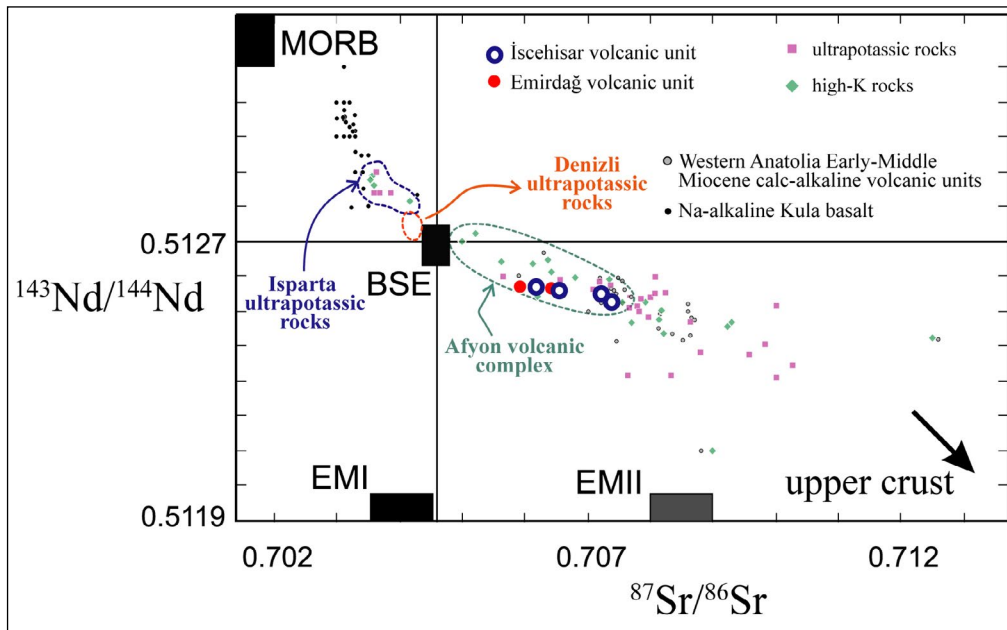


Figure 7- ⁸⁷Sr/⁸⁶Sr versus ¹⁴³Nd/¹⁴⁴Nd isotope diagram for the İscehisar and Emirdağ volcanic units. Comparisons with other rocks outcropping in western Anatolia included on the diagram. Isotope ratios were taken from Aldanmaz et al. (2000), Akal (2008), Alıcı et al. (1998, 2002) Chakrabarti et al. (2012), Çoban et al. (2012), Dilek and Altunkaynak (2010), Güleç (1991), Innocenti et al. (2005), Karaoğlu et al. (2010) and Prelević et al. (2012). MORB: mid-ocean ridge basalt, BSE: bulk silicate earth, EMI: enriched mantle I, EMII: enriched mantle II.

lesser amount of samples are alkaline in character. In terms of the K₂O content of volcanic rocks, they have high-K calc-alkaline and shoshonitic character. The İscehisar volcanic unit have variable compositions from basaltic trachyandesite through trachyte and trachydacite. The İscehisar samples have alkaline and shoshonitic character and display geochemically different trends with respect to the Emirdağ volcanic samples. Primitive mantle and Chondrite normalized spider diagrams show that the İscehisar and Emirdağ volcanic units have variable degrees of enrichment and/or depletion in some elements.

Somewhat variable mineralogical and geochemical features, varying from basic to acidic members, of the İscehisar and Emirdağ volcanic units indicate that these units have experienced fractional crystallisation and contamination (Figure 8). La/Sm increases with Th/Nb in the Emirdağ volcanic unit, while significant correlation in these ratios is absent in the İscehisar volcanic unit. Increasing Th/Nb in the Emirdağ volcanic unit indicates the role of crustal contamination or magma mixing processes. On the other hand, increasing La/Sm with almost constant Th/Nb imply the prominent role of fractional

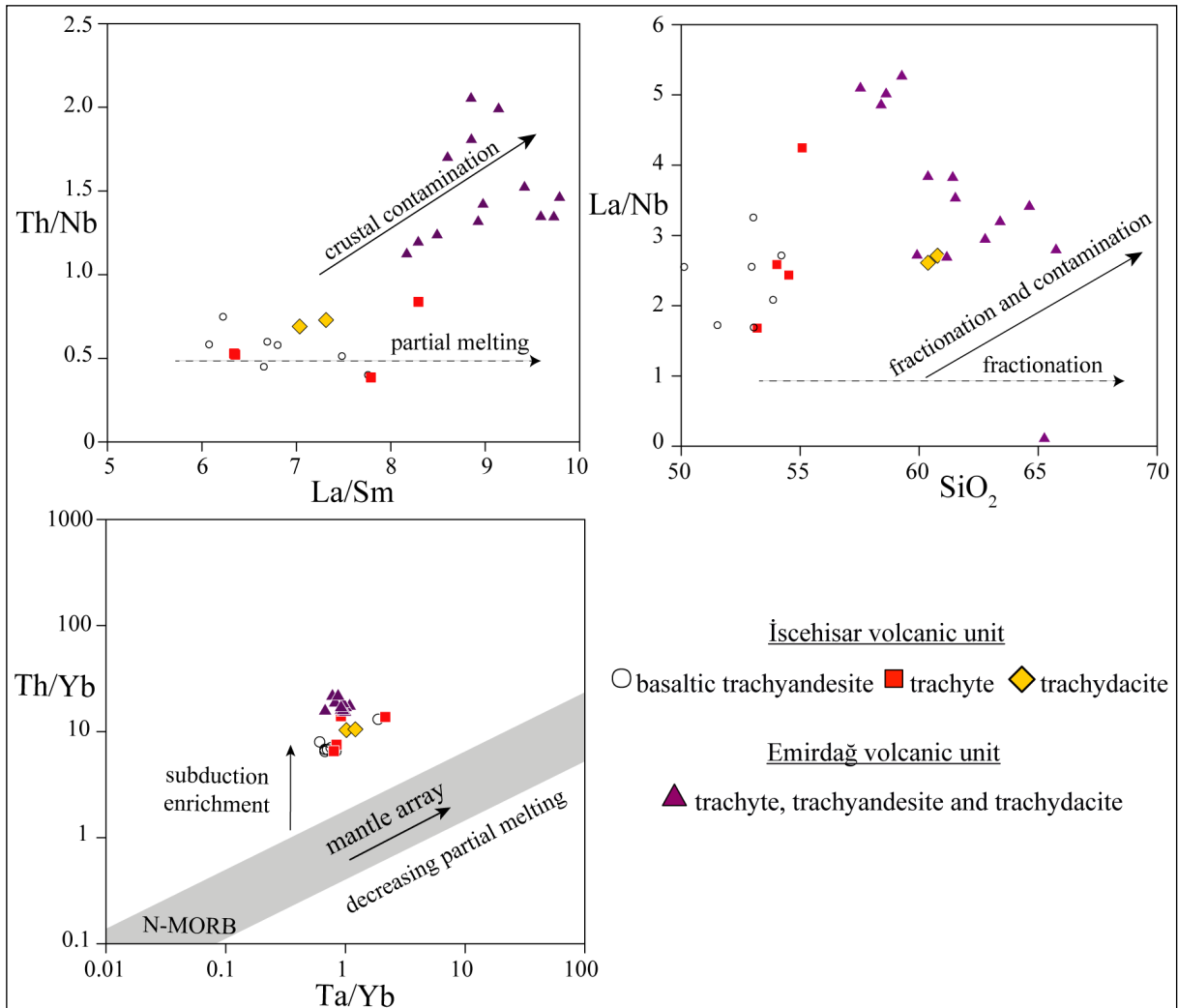


Figure 8- Variations diagrams for a) Th/Nb against La/Sm, (b) La/Nb against SiO₂ and c) Th/Yb against Ta/Yb.

crystallisation or different degrees of partial melting processes, leading to the transition from basaltic trachyandesite to trachydacite compositions in the İscehisar volcanic unit. The positive trend on the La/Nb versus SiO₂ variation diagram shows that the Emirdağ and İscehisar volcanic units were affected by fractional crystallization and fractional crystallisation-crustal contamination during their formation. Plagioclase and matrix inclusions within biotites, and zoned and spongy cellular texture plagioclase phenocrysts in the Emirdağ lava samples and matrix inclusions in pyroxene and olivine phenocrysts in the İscehisar lava samples indicate the presence of magma mixing processes. Clinopyroxene needles mantled by quartz phenocrysts in the lava samples of the İscehisar volcanic unit can be interpreted as a marker for magma mixing processes (Dedeoğlu and Yılmaz, 2016).

When all data are evaluated together, contribution of mantle and crustal sources at varying degrees occurred during formation of the Emirdağ and İscehisar volcanic units. All volcanic units have low to moderate ⁸⁷Sr/⁸⁶Sr, Nb/U and Ce/Pb, and relatively high ¹⁴³Nd/¹⁴⁴Nd ratios. Enrichment of large-ion lithophile elements in subduction-related volcanic rocks is expected in addition to enrichment of Pb. However, the Emirdağ and İscehisar volcanic units do not appear to have enriched in Pb content identical to subduction setting, and even depletion of Pb in some samples is observed on multi-element spider diagrams. Although a negative Pb anomaly indicates asthenospheric mantle source, the behaviour of elements in the volcanic units support addition of subduction-related metasomatic solutions infiltrated into an enriched mantle source. The higher Mg# values

in the İncehisar volcanic unit compared to the Emirdağ volcanic unit indicates more mantle input during the formation of İncehisar volcanic unit. The increasing Th/Yb ratios indicate progressively metasomatized mantle source by subduction-related solutions. The higher Th/Nb ratios in the İncehisar volcanic unit compared to the Emirdağ volcanic unit imply that the subduction-related contribution occurred at higher rates during its formation.

8. Tectono-Magmatic Evolution

Geodynamic models involving orogenic collapse and associated lithospheric delamination (Aldanmaz et al., 2000; Dilek and Altunkaynak, 2009), slab roll-back resulting in mantle upwelling, and subducted lithospheric thinning and subsequent slab tearing have been proposed for the geodynamic environment that controlled Anatolian magmatism since Late Oligocene. As partial melting of the mantle wedge showing advanced degree of metasomatism due to infiltration of solutions and melts derived from the rolled-back slab causes development of K-rich magma (Lustrino et al., 2011 and references therein). Slab tear causes upwelling of juvenile, sub-slab asthenospheric mantle (Gasparon et al., 2009; Miller and Lee, 2008; Russo et al., 2010). The upwelled asthenospheric mantle may be partially melted itself, or may cause partial melting of the lithospheric mantle and lower crust owing to the induced high heat flow. In this scenario, nature of magmatism passes from high-K calc-alkaline to Na-rich alkaline in the advanced stages of slab tear (Doglioni et al., 2002; Tokçaer et al., 2005).

Early-middle Miocene magmatic belts in western Anatolia are represented by calc-alkaline, shoshonitic and ultrapotassic rocks with different compositions. Miocene magmatic rocks are locally observed as volcanic assemblages represented by the association of coeval calc-alkaline and mildly alkaline rocks. The distribution of these rocks is typically restricted to the Neogene basins, suggested to have developed under the NE-SW-directed extensional regime (Erkül et al., 2005a, b; Altunkaynak et al., 2010; Ersoy et al., 2008). During the early-middle Miocene, calc-alkaline volcanism in western Anatolia were resulted from the interaction between lower crust and metasomatized lithospheric mantle-derived magmas. These processes inferred to have been active since 12.2 Ma (Erkül et al., 2013). After the volcanic quiescence until 8.5 Ma,

alkaline volcanism with geochemical signatures of asthenospheric contribution around Denizli, Selendi and Kula became active and this activity continued to the present day (Alicı et al., 2002; Ersoy et al., 2011; Innocenti et al., 2005; Yılmaz, 2010).

Calc-alkaline, shoshonitic and ultrapotassic rock assemblages occurred during 20 to 16 Ma are exposed around Eskişehir, Afyon and Isparta. Calc-alkaline volcanic rocks crop out in a NW-SE-trending belt from Eskişehir towards Emirdağ (Figure 9a). Along this belt, widespread calc-alkaline pyroclastic deposits are accompanied by alkali trachydacites, trachytes, basaltic trachyandesites, lamprophyres and lamproites. All volcanic rocks to the south of Emirdağ and İncehisar have alkaline character. Lamproites emplaced after 12 Ma display geochemical evidences of asthenospheric input (Prelević et al., 2015) and this contribution in volcanic units increased in Senirkent, Isparta and Bucak (Çoban and Flower, 2006) towards south (Dilek and Altunkaynak, 2010; Elitok, 2019). The Emirdağ and İncehisar volcanic units can be accounted for the final products of orogenic volcanism developed within this belt. Calc-alkaline volcanism in western Anatolia is considered to have developed under the NE-SW oriented extensional regime since early Miocene. The extensional regime in western Anatolia was widely accepted to have occurred in response to roll-back of the subducting African oceanic lithosphere (Brun and Sokoutis, 2010; Gessner et al., 2013; Jolivet et al., 2013). Middle Miocene shoshonitic volcanism derived from lithospheric mantle and crustal sources around Emirdağ and İncehisar regions along with the roll-back of the subducting oceanic slab. The roll-back of the subducting slab triggered the upwelling of the asthenosphere as a heat source in the overlying mantle wedge, causing elevation and expansion in the crust. The rise of the asthenosphere during subduction processes might have caused partial melting of the metasomatized mantle wedge. The upwelling of asthenosphere also caused partial melting of the lower crust (Figure 9b). Coeval lithospheric mantle and crustal derived magmas may have mixed with each other at different rates (Figure 9c). Continental crust-derived melts at the initial stage were emplaced in the upper crust and are inferred to have formed the widespread Seydiler Ignimbrite associated with a caldera system. In advancing stages, the lithospheric mantle and lower crust-derived magmas might have mixed with each other. When compared to the

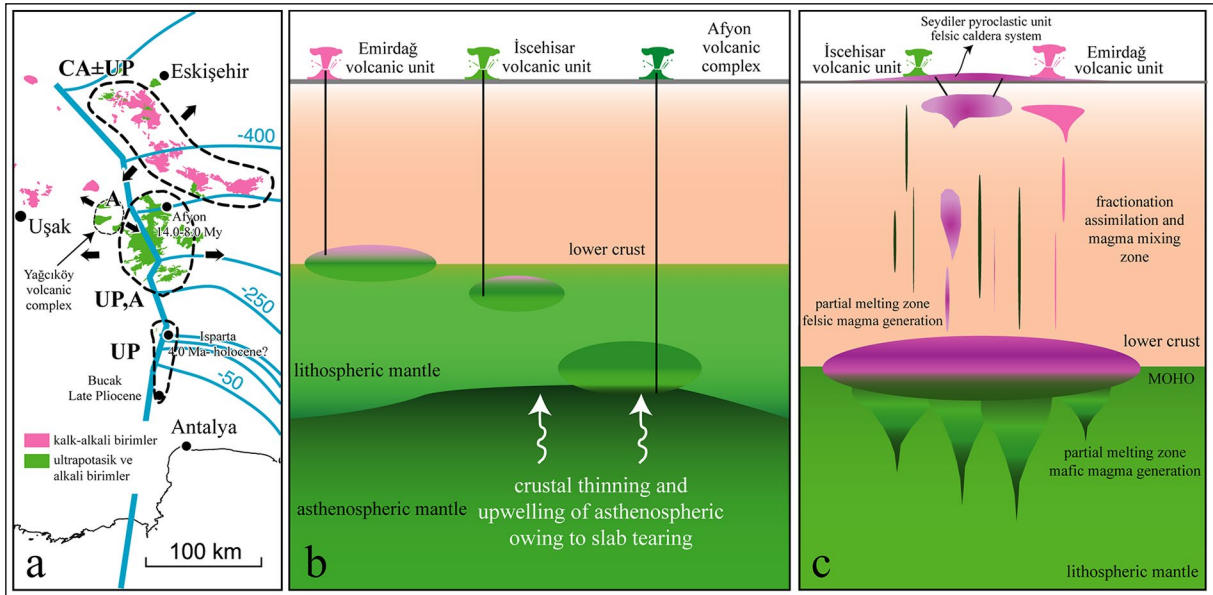


Figure 9- a) Map showing distribution of Miocene volcanic complexes outcropping between Afyon-Eskişehir (areas bounded by dashed lines). Yağcıköy volcanic complex comprises alkaline rocks located west of the Afyon volcanic complex and is outside the N-S striking emplacement axis (Erkül et al., 2019). Thin blue lines represent contours showing depth of the upper surface of the subducted lithosphere slab (depth in km). Thick blue line is equivalent to the projection on the surface of the edge of the torn slice. Data were taken from Biryol et al. (2011). CA: calc-alkaline, A: alkaline, UP: ultrapotassic volcanic rock assemblages. b) Schematic section showing location of the magma chamber forming the Emirdağ, İncehisar and Afyon volcanic units. c) Schematic section showing mixing of magmas in the lithospheric mantle and lower crust, fractionation and contamination by the upper crust.

İncehisar volcanic unit, crustal contribution to the Emirdağ volcanic unit is greater and the İncehisar volcanic unit appear to have greater contribution from metasomatized lithospheric mantle under the extensional regime. This extensional regime occurred immediately before tearing of the subducting oceanic slab. Oceanic slab tearing event is represented by voluminous alkaline volcanic rocks within the Afyon volcanic complex.

9. Conclusions

(1) Coeval calc-alkaline and alkaline volcanism occurs in the around Emirdağ and İncehisar areas. Calc-alkaline volcanism has dominantly trachydacite composition in Emirdağ and surroundings. Alkaline volcanism begins with basaltic trachyandesite and ends with trachydacite in İncehisar and surroundings.

(2) Geochemical data show that the Emirdağ and İncehisar volcanic units were affected by crustal contamination, fractional crystallisation and magma

mixing processes. The magma mixing processes and crustal contamination was greater in the Emirdağ volcanic unit compared to the İncehisar volcanic unit.

(3) The extensional regime that has been active in the middle Miocene might have been caused by upwelling of the lithospheric mantle metasomatized during pre-Miocene former subduction events. Interaction of mantle- and crust-derived magmas at transition from slab roll-back to tearing stages resulted in a shift in geochemical character of the volcanism from calc-alkaline to alkaline character. The Emirdağ and İncehisar volcanic units are inferred to represent the transitional volcanism between two geodynamic episodes.

Acknowledgements

This study was supported by the Akdeniz University Scientific Research Projects Coordination Unit (project number FYL-2015-823).

References

- Agostini, S., Ryan, J.G., Tonarini, S., Innocenti, F. 2008. Drying and dying of a subducted slab: Coupled Li and B isotope variations in western Anatolia Cenozoic Volcanism. *Earth and Planetary Science Letters* 272 (1-2), 139-147.
- Akal, C. 2003. Mineralogy and geochemistry of melilite leucitites, Balçıkhisar, Afyon (Turkey). *Turkish Journal of Earth Sciences* 12 (3), 215-239.
- Akal, C. 2008. K-richterite–olivine–phlogopite–diopside–sanidine lamproites from the Afyon volcanic province, Turkey. *Geological Magazine* 145 (4), 570-585.
- Aldanmaz, E., Pearce, J.A., Thirlwall, M.F., Mitchell, J.G. 2000. Petrogenetic evolution of Late Cenozoic, post-collision volcanism in western Anatolia, Turkey. *Journal of Volcanology and Geothermal Research* 102 (1), 67- 95.
- Alici, P., Temel, A., Gourgaud, A., Kieffer, G., Gündoğdu, M.N. 1998. Petrology and geochemistry of potassic rocks in the Gölcük area (Isparta, SW Turkey): Genesis of enriched alkaline magmas. *Journal of Volcanology and Geothermal Research* 85, 423-446.
- Alici, P., Temel, A., Gourgaud, A. 2002. Pb–Nd–Sr isotope and trace element geochemistry of Quaternary extension-related alkaline volcanism: A case study of Kula region (western Anatolia), Turkey. *Journal of Volcanology and Geothermal Research* 115 (3–4), 487–510.
- Altunkaynak, S., Rogers, N.W., Kelley, S.P. 2010. Causes and effects of geochemical variations in late Cenozoic volcanism of the Foça volcanic centre, NW Anatolia, Turkey. *International Geology Review* 52 (4–6), 579–607.
- Aydar, E. 2003. Les lamprophyres du stratovolcan d’Afyon, Anatolie de l’Ouest, Turquie: Description et genèse. *Comptes Rendus Geosciences* 335 (3), 279-288.
- Aydar E., Bayhan H. 1995. Le volcanisme alcalin d’Afyon, Anatolie de l’ouest, Turquie: Approche volcanologique et pétrologique. *Bulletin Section Volcanologique Soc Géol France* 36, 1-5.
- Aydar, E., Bayhan, H., Zimitoğlu, O. 1996. Afyon stratovolkanının volkanolojik ve petrolojik gelişiminin incelenmesi. *Yerbilimleri* 18, 87-107.
- Aydar, E., Bayhan, H., Gourgaud, A. 1998. Köroğlu caldera, mid-west Anatolia, Turkey: Volcanological and magmatological evolution. *Journal of Volcanology and Geothermal Research* 85 (1), 83-98.
- Besang, C., Eckhardt, F.J., Harre, W., Kreuzer, H. Müller, P. 1977. Radiometrische altersbestimmungen an Neogenen eruptivgesteinen der Türkei. *Geologisches Jahrbuch* 25, 3-36.
- Biryol, C.B., Beck, S.L., Zandt, G., Özacar, A.A. 2011. Segmented African lithosphere beneath the Anatolian region inferred from teleseismic P-wave tomography. *Geophysical Journal International* 184 (3) 1037-1057.
- Boynton, W.V. 1984. Cosmochemistry of the rare earth elements; meteorite studies. Elsevier 63-114, Amsterdam.
- Brun, J. P., Sokoutis, D. 2010. 45 m.y. of Aegean crust and mantle flow driven by trench retreat. *Geology* 38, 815–818.
- Chakrabarti, R., Basu, A., Ghatak, A. 2012. Chemical geodynamics of western Anatolia. *International Geology Review* 54 (2), 227-248.
- Çoban, H., Flower, M.F. 2006. Mineral phase compositions in silica undersaturated ‘leucite’ lamproites from the Bucak area, Isparta, SW Turkey. *Lithos* 89 (3), 275- 299.
- Çoban, H., Karacık, Z., Ece, Ö.I. 2012. Source contamination and tectonomagmatic signals of overlapping Early to Middle Miocene orogenic magmas associated with shallow continental subduction and asthenospheric mantle. *Lithos* 140, 119-141.
- Dedeoğlu, D., Yılmaz, K. 2016. Geochemistry of lamprophyres in Karakaya (İscehisar, Afyon), western Anatolia, Turkey. *IOP Conference Series, Earth and Environmental Science* 44 (4).
- Dewey J.F. 1988. Extensional collapse of orogens. *Tectonics* 7, 1123-1139.
- Dilek, Y., Altunkaynak, Ş. 2009. Geochemical and temporal evolution of Cenozoic magmatism in western Turkey: mantle response to collision, slab breakoff and lithospheric tearing in an orogenic belt. *Geological Society of London Special Publications* 311, 1, 213-233.
- Dilek, Y., Altunkaynak, Ş. 2010. Geochemistry of Neogene–Quaternary alkaline volcanism in western Anatolia, Turkey and implications for the Aegean mantle. *International Geology Review* 52 (4-6), 631-655.
- Dogliani, C., Agostini, S., Crespi, M., Innocenti, F., Manetti, P., Riguzzi, F., Savaşın, Y., 2002. On the extension in western Anatolia and the Aegean sea. In: (Eds.) Gideon Rosenbaum and Gordon Lister, *Journal of the Virtual Explorer* 8, DOI: 10.3809/jvirtex.2002.00049.
- Doğan Kūlahcı, G.D., Temel, A., Gourgaud, A., Demirbağ, H. 2016. Afyon volkanik kayaçlarının (Batı Anadolu, Türkiye) mineralojik-petrografik özellikleri ve P-T Hesaplamaları. *Yerbilimleri/*

- Hacettepe Üniversitesi Yerbilimleri Uygulama ve Araştırma Merkezi Dergisi 36 (3), 137-162.
- Elitok, Ö. 2019. Geology and petrology of the potassic and ultrapotassic rocks from the northern part of Senirkent (Isparta-SW Turkey): Evidence of magma-carbonate wall-rock interactions. *Arabian Journal of Geosciences* 12 (9).
- Elitok, Ö., Özgür, N., Druppel, K., Dilek, Y., Platevoet, B., Guillou, H., Poisson, A., Scaillet, S., Satir, M., Siebel, W., Bardintzeff, J.M., Deniel, C., Yılmaz, K. 2010. Origin and geodynamic evolution of Late Cenozoic potassium-rich volcanism in the Isparta area, southwestern Turkey. *International Geology Review* 52 (4-6), 454-504.
- Erkül, F., Helvacı, C., Sözbilir, H. 2005a. Evidence for two episodes of volcanism in the Bigadiç borate basin and tectonic implications for western Turkey. *Geological Journal* 40 (5), 545-570.
- Erkül, F., Helvacı, C., Sözbilir, H. 2005b. Stratigraphy and geochronology of the Early Miocene volcanic units in the Bigadiç borate basin, western Turkey. *Turkish Journal of Earth Sciences* 14 (3), 227-253.
- Erkül, F., Helvacı, C., Sözbilir, H. 2006. Olivine basalt and trachyandesite peperites formed at the subsurface/surface interface of a semi-arid lake: An example from the Early Miocene Bigadiç basin, western Turkey. *Journal of Volcanology and Geothermal Research* 149 (3-4), 240-262.
- Erkül, F., Erkül, S. T., Ersoy, Y., Uysal, İ., Klötzli, U. 2013. Petrology, mineral chemistry and Sr-Nd-Pb isotopic compositions of granitoids in the central Menderes metamorphic core complex: Constraints on the evolution of Aegean lithosphere slab. *Lithos* 180-181, 74-91.
- Erkül, F., Çolak, C., Erkül, S.T., Varol, E. 2019. Geology and geochemistry of the Middle Miocene Yağcıköy volcanic complex, western Turkey: Wide-rift alkaline volcanism associated with incipient stages of slab tearing. *Journal of Asian Earth Sciences* 179, 112-126.
- Ersoy, Y., Helvacı, C., Sözbilir, H., Erkül, F., Bozkurt, E. 2008. A geochemical approach to Neogene-Quaternary volcanic activity of western Anatolia: An example of episodic bimodal volcanism within the Selendi Basin, Turkey. *Chemical Geology* 255 (1-2), 265-282.
- Ersoy, Y.E., Helvacı, C., Palmer, M.R. 2011. Petrogenesis of the Neogene volcanic units in the NE-SW-trending basins in western Anatolia, Turkey. *Contributions to Mineralogy and Petrology* 163(3), 379-401.
- Foley, S., Venturelli, G., Green, D.H., Toscani, L. 1987. The ultrapotassic rocks: Characteristics, classification and constraints for petrogenetic models. *Earth Science Reviews* 24 (2), 81-134.
- Francalanci, L. 1990. Tertiary-Quaternary alkaline magmatism of the Aegean western Anatolian area: A petrological study in the light of new geochemical and isotopic data. *International Earth Sciences Colloquium on the Aegean Region 385-396*, 1-6 October, Dokuz Eylül University, İzmir.
- Francalanci, L., Innocenti, F., Manetti, P., Savaşçın, M.Y. 2000. Neogene alkaline volcanism of the Afyon-Isparta area, Turkey: Petrogenesis and geodynamic implications. *Mineralogy and Petrology* 70 (3-4), 285-312.
- Gasparon, M., Rosenbaum, G., Wibranjs, J.R., Manetti, P. 2009. The transition from subduction arc to slab tearing: Evidence from Capraia Island, northern Tyrrhenian Sea. *Journal of Geodynamics* 47 (1), 30-38.
- Gessner, K., Gallardo, L. A., Markwitz, V., Ring, U., Thomson, S. N. 2013. What caused the denudation of the Menderes Massif: Review of crustal evolution, lithosphere structure, and dynamic topography in southwest Turkey. *Gondwana Research*, 24, 243-274.
- Güleç, N. 1991. Crust-mantle interaction in western Turkey: Implications from Sr and Nd isotope geochemistry of Tertiary and Quaternary volcanics. *Geological Magazine* 128 (5), 417-435.
- Innocenti, F., Agostini, S., Di Vincenzo, G., Doglioni, C., Manetti, P., Savaşçın, M.Y., Tonaini, S. 2005. Neogene and Quaternary volcanism in western Anatolia: magma sources and geodynamic evolution. *Marine Geology* 221 (1), 397-421.
- Irvine, T.N., Baragar, W.R.A. 1971. A Guide to the Chemical Classification of the Common Volcanic Rocks. *Canadian Journal of Earth Science* 8, 523-548.
- Janousek, V., Farrow, C. M., Erban, V. 2006. Interpretation of whole-rock geochemical data in igneous geochemistry: Introducing geochemical data Toolkit (*GCDkit*). *Journal of Petrology* 47 (6), 1255-1259.
- Jolivet, L., Faccenna, C., Huet, B., Labrousse, L., Le Pourhiet, L., Lacombe, O., Lecomte, E., Burov, E., Denéle, Y., Brun, J.-P., Philippon, M., Paul, A., Salaün, G., Karabulut, H., Piromallo, C., Monié, P., Gueydan, F., Okay, A.I., Oberhänsli, R., Pourteau, A., Augier, R., Gadenne, L., Driussi, O. 2013. Aegean tectonics: Strain localisation, slab tearing and trench retreat. *Tectonophysics* 597-598, 1-33.

- Karaoğlu, Ö., Helvacı, C. 2012. Structural evolution of the Uşak-Güre supra-detachment basin during Miocene extensional denudation in western Turkey. *Journal of the Geological Society* 169 (5), 627-642.
- Karaoğlu, Ö., Helvacı, C. 2014. Isotopic evidence for a transition from subduction to slab-tear related volcanism in western Anatolia, Turkey. *Lithos* 192-195, 226-239.
- Karaoğlu, Ö., Helvacı, C., Ersoy, Y. 2010. Petrogenesis and $^{40}\text{Ar}/^{39}\text{Ar}$ geochronology of the volcanic rocks of the Uşak-Güre basin, western Turkey. *Lithos* 119 (3-4), 193-210.
- Keller, J. 1983. Potassic lavas in the orogenic volcanism of the Mediterranean area. *Journal of Volcanology and Geothermal Research* 18 (1), 321-335.
- Keller, J., Villari, L. 1972. Rhyolitic ignimbrites in the region of Afyon (Central Anatolia). *Bulletin Volcanologique* 36 (2), 342-358.
- Köksal, S., Göncüoğlu, M.C. 2008. Sr and Nd isotopic characteristics of some S-, I and A-type granitoids from Central Anatolia. *Turkish Journal of Earth Sciences* 17 (1), 111-127.
- Kumral, M., Çoban, H., Gedikoğlu, A., Kılınç, A. 2006. Petrology and geochemistry of augite trachytes and porphyritic trachytes from the Gölcük volcanic region, Isparta, SW Turkey: A case study. *Journal of Asian Earth Sciences* 27 (5), 707- 716.
- Le Bas, M.J., Le Maitre, R.W., Streckeisen, A., Zanettin, B. 1986. A chemical classification of volcanic rocks based on the total alkali-silica diagram. *Journal of Petrology* 27 (3), 745-750.
- Lustrino, M., Duggen, S., Rosenberg, C.L. 2011. The central-western Mediterranean: Anomalous igneous activity in an anomalous collisional tectonic setting. *Earth-Science Reviews* 104, 1-40
- Mahatsente, R., Alemdar, S., Çemen, İ. 2017. Effect of slab-tear on crustal structure in Southwestern Anatolia. *Active Global Seismology* 103-119.
- Metin, S., Genç, Ş., Bulut, V. 1987. Afyon ve dolayının jeolojisi. Maden Tetkik ve Arama Genel Müdürlüğü Raporu No: 8103, Ankara (unpublished).
- Miller, M.S., Lee, C.-T.A. 2008. Possible chemical modification of oceanic lithosphere by hotspot magmatism seismic evidence from the junction of Ninety East Ridge and the Sumatra-Andamanarc. *Earth Planetary and Science Letters* 265, 386-395.
- MTA, 2002. 1/500.000 ölçekli jeoloji haritası. Maden Tetkik ve Arama Genel Müdürlüğü, Ankara.
- Peccerillo, A., Taylor, S.R. 1976. Geochemistry of Eocene calc-alkaline volcanic rocks from the Kastamonu area, Northern Turkey. *Contributions to Mineralogy and Petrology* 58, 63-81.
- Platevoet, B., Scaillet, S., Guillou, H., Blamart, D., Nomade, S., Massault, M., Poisson, A., Elitok, Ö., Özgür, N., Yağmurlu, F., Yılmaz, K. 2008. Pleistocene eruptive chronology of the Gölcük volcano, Isparta angle, Turkey. *Quaternaire. Revue de l'Association Française Pour L'étude du Quaternaire* 19 (2), 147-156.
- Portner, D. E., Delph, J. R., Biryol, C. B., Beck, S. L., Zandt, G., Özacar, A.A., Sandvol, E., Turkelli, N. 2018. Subduction termination through progressive slab deformation across eastern Mediterranean subduction zones from updated P-wave tomography beneath Anatolia. *Geosphere* 14 (3), 907-925.
- Prelević, D., Akal, C., Romer, R.L., Foley, S.F. 2010. Lamproites as indicators of accretion and/or shallow subduction in the assembly of Southwestern Anatolia, Turkey. *Terra Nova* 22 (6), 443-452.
- Prelević, D., Akal, C., Foley, S.F., Romer, R.L., Stracke, A., Van Den Bogaard P. 2012. Ultrapotassic mafic rocks as geochemical proxies for postcollisional dynamics of orogenic lithospheric mantle: the case of Southwestern Anatolia, Turkey. *Journal of Petrology* 53 (5), 1019-1055.
- Prelević, D., Akal, C., Romer, R. L., Mertz-Kraus, R., Helvacı, C. 2015. Magmatic response to slab tearing: Constraints from the Afyon alkaline volcanic complex, western Turkey. *Journal of Petrology* 56 (3), 527-562.
- Russo, R.M., Gallego, A., Comte, D., Mocanu, V.I., Murdie, R.E., Van Decar, J.C. 2010. Source-side shear wave splitting and upper mantle flow in the Chile Ridge subduction region. *Geology* 38, 707-710.
- Savaşçın, Y., Güleç, N. 1990. Relationship between magmatic and tectonic activities in western Turkey. *International Earth Sciences Colloquium on the Aegean Region* 300-313, 1-6 October, Dokuz Eylül University, İzmir.
- Savaşçın, M.Y., Oyman, T. 1998. Tectono-magmatic evolution of alkaline volcanics at the Kırka-Afyon-Isparta structural trend, SW Turkey. *Turkish Journal of Earth Sciences* 7 (3), 201-214.
- Seghedi, I., Helvacı, C. 2016. Early Miocene Kırka-Phrigan Caldera, western Turkey (Eskisehir province), preliminary volcanology, age and geochemistry data. *Journal of Volcanology and Geothermal Research* 327, 503-519.

- Seyitođlu, G., Scott, B.C. 1996. The age of the Alařehir graben (west Turkey) and its tectonic implications, *Geological Journal* 31, 1-11.
- Soder, C. 2017. Geochemistry and petrology of lamprophyres from the Hellenides and the European Variscides. MsC Thesis, Heidelberg University, 185s.
- Sun, S.S., McDonough, W.S. 1989. Chemical and isotopic systematics of oceanic basalts: Implications for mantle composition and processes. *Geological Society of London Special Publications* 42 (1), 313-345.
- Sunder, M.S. 1980. Geochemistry of the Sarıkaya borate deposits (Kırka-Eskiřehir). *Bulletin of the Geological Society of Turkey* 2, 19-34.
- Tokçær, M., Agostini, S., Savaşçın, M.Y., 2005. Geotectonic setting and origin of the youngest Kula volcanics (western Anatolia), with a new emplacement model. *Turkish Journal of Earth Sciences* 14, 145–166.
- Tonarini, S., Agostini, S., Innocenti, F., Manetti, P. 2005. Delta11B as tracer of slab dehydration and mantle evolution in western Anatolia Cenozoic Magmatism. *Terra Nova*, 17 (3), 259-264.
- Yađmurlu, F., Savaşçın, Y., Ergün, M. 1997. Relation of alkaline volcanism and active tectonism within the evolution of the Isparta Angle, SW Turkey. *The Journal of Geology* 105 (6), 717-728.
- Yılmaz, K. 2010. Origin of anorogenic ‘lamproite-like’ potassic lavas from the Denizli region in western Anatolia extensional province, Turkey. *Mineralogy and Petrology* 99 (3), 219–239.

